Laboratory studies of uv emissions of H_2 by electron impact. The Werner- and Lyman-band systems

J. M. Ajello and S. K. Srivastava
Jet Propulsion Laboratory, California Institute of Technology, Pasadena, California 91109

Yuk L. Yung
Division of Geological & Planetary Sciences, California Institute of Technology, Pasadena, California 91125

(Received 1 October 1981)

We report a laboratory measurement of absolute emission cross sections of both the Lyman bands ($B\,^1\Sigma_u^+ \rightarrow X\,^1\Sigma_g^+$) and Werner bands ($C\,^1\Pi_u \rightarrow X\,^1\Pi_g^+$) of H_2 by electron impact over the energy range from threshold to 400 eV with the same optical system. We find the emission cross section for the $B\,^1\Sigma_u^+ \rightarrow X\,^1\Sigma_g^+$ transition at 100 eV to be $(3.55\pm0.8)\times10^{-17}$ cm^2 (2.7×10^{-17} cm^2, direct excitation, 0.85×10^{-17} cm^2, cascading) and the emission cross section for the $C\,^1\Pi_u \rightarrow X\,^1\Sigma_g^+$ transition at 100 eV to be $(3.1\pm0.6)\times10^{-17}$ cm^2 (cascading is estimated to be not present). The cross-section ratio Q_C/Q_B for direct excitation is 1.21 ± 0.30 at 300 eV in excellent agreement with published values for this ratio from theoretical calculations and experimental data of the optical oscillator strengths. We measure the cross section for cascading to the B state to be $24\pm10\%$ of the total emission cross section both at 100 and 300 eV. We show that cascading increases to $51\pm20\%$ of the total cross section of the B state at 20 eV. The vibrational population distribution of the B state is found to be a function of electron-impact energy as the importance of cascading relative to direct excitation changes with electron-impact energy.

I. INTRODUCTION

The H_2 molecule is important since it is the simplest molecule to be studied from a theoretical point of view and it is the most abundant molecule in the universe. Unfortunately there is sparse laboratory data available to deal with the emissions of the two strongest transitions of H_2 which occur in the uv: the Lyman-band system ($B\,^1\Sigma_u^+ \rightarrow X\,^1\Sigma_g^+$) and the Werner-band system ($C\,^1\Pi_u \rightarrow X\,^1\Sigma_g^+$). Most of our knowledge of electron-impact emission cross sections of H_2 depends on the validity of the Born-Bethe approximation coupled with optical oscillator strength measurements[1] or *ab initio* theoretical calculations, which do not allow for cascade.[2–5] The one experimental emission cross-section determination[6] of the Werner bands differs by nearly a factor of 2 at 100 eV from the theoretical estimates. This situation has become untenable with the recent observations of intense H_2 aurora in the uv by Voyager and International Ultraviolet Explorer.[7–10] These spacecraft data require an accurate set of laboratory cross sections for properly modeling the auroral precipitating flux of electrons into the atmosphere of Jupiter.[10]

The first experimental determination of the emission cross section of either of these band systems was accomplished by Stone and Zipf.[6] They measured absolute cross sections of about ten rotational lines of the Werner bands. From their cross sections of rotational lines it is possible to calculate a total electronic cross section based on transition probabilities and Honl-London factors. We find a value of 5.3×10^{-17} cm^2 at 100 eV. This value contrasts by nearly a factor of 2 from deHeer and Carriere's[1] experimental relative-cross-section measurement which utilizes the Born-Bethe approximation and absorption oscillator strengths at high energy for normalization. Fortunately, the experimental[11] and theoretical oscillator strengths[12] used in the normalization are in close agreement (20%) and lead to an acceptable range of values at 100 eV of $(3.2\pm0.4)\times10^{-17}$ cm^2.

At the same time there has not been any experimental measurement of the emission cross section of the entire Lyman-band system. Malcolm *et al.*[13] have measured the excitation function for the B state and have normalized this function to

the semiempirical data of Gerhardt.[14] Srivastava and Jensen[15] have measured the direct-excitation cross section of the B state by an electron scattering experiment over the electron-impact energy range 0—60 eV. However, the B state contains a large cascade contribution, particularly from the transition $E,F\,^1\Sigma_g^+ \rightarrow B\,^1\Sigma_u^+$. Estimates for this contribution at 100 eV based on theory[4,16] and an experimental measurement by Watson and Anderson[17] (and references cited therein) range from 6 to 25% of the total B state emission cross section. McConkey[18] has recently measured the excitation function of two rotational lines of the B state and has used this result together with the results of Gerhardt[14] to determine the direct cross section of the entire band system. At this juncture the *ab initio* theoretical approaches for the B-state direct-excitation cross section are larger than the experimental electron scattering result and the cross-section result of McConkey; for example, the theoretical and experimental results differ by a factor of 2 at about 40 eV.[5]

Our plan is to study the vacuum ultraviolet (vuv) electron-impact induced-fluorescence emissions of H_2 from both band systems from 120 to 170 nm with the same optical system composed of a photomultiplier and a spectrometer so that additional uncertainty in calibration is eliminated. With this approach at any one electron-impact energy we will detect, simultaneously, as a function of wavelength, about 80% of the Lyman-band system composed of both direct and cascade contributions and about 15% of the Werner-band system, where cascading is small,[19] and for which the remaining 85% of the band system can be readily synthesized from transition probabilities.[12] The electron-impact induced-fluorescence spectra at 20, 50, 100, and 300 eV as measured in this laboratory are compared to synthetic spectra by a least-squares technique that treats the relevant cross sections as unknown parameters. The accompanying Lyman-α emission produced by dissociative excitation of H_2 serves as a calibration standard.[20] Our final goal is to compare various theoretical and experimental estimates of the cross section.

II. EXPERIMENTAL

A detailed description of the experimental apparatus is presented in Ajello and Srivastava[21] hereafter referred to as paper I. The apparatus consists of an electron-impact collision chamber in tandem with a uv spectrometer. A collimated beam of electrons is generated by an electron gun whose kinetic energy can be varied from 1 eV to a few keV. The energy spread of the beam is estimated to be about 0.5 eV and the absolute energy scale is accurate to 1 eV. This beam of electrons is crossed with a beam of gas formed by a capillary which produces a background gas pressure of 2×10^{-5} Torr. Inelastic electron-molecule collisions lead to emission of photons. At an angle of 90° with respect to the direction of the electron beam the photons enter into the uv spectrometer, which consists of 20-cm focal length osmium-coated holographic concave grating that operates in the normal incidence mode. The grating can be rotated around a vertical axis; thus a spectral region between 50 and 500 nm can be scanned. The photon detector for the study of vacuum uv spectral region was an EMI photomultiplier with a CsI photocathode and MgF window. The usual linearity checks of signal intensity versus current and pressure were made to demonstrate the absence of secondary processes at the energies studied.

The entire optical system was calibrated on a relative basis from 115 to 180 nm using the molecular branching-ratio technique described by Mumma[22] and Mumma and Zipf[23] with the gas N_2. The relative optical calibration is shown in Fig. 1. Its accuracy is 15% in the spectral range 120—180 nm and estimated to be 30% in the spectral range 115—120 nm. The quantitative results presented in this study utilize the spectral range 120—180 nm. Furthermore an absolute calibration of the optical system was performed as described in paper I by measuring the area under the Lyman-α feature when excited by 100-eV electrons on H_2. The Lyman-α emission cross section from H_2 has been accurately determined to be 1.2×10^{-17} cm^2 at 100 eV by several experimenters.[20] In addition, Mumma and Zipf[20] have measured the Lyman-α emission cross section from H_2 to be 6×10^{-18} cm^2 at 300 eV. We use this value for an absolute calibration at 300 eV. The one standard deviation uncertainty of an H_2 emission cross-section determination, uncorrected for cascade, is 20% in the 120—180-nm spectral range.

The spectrometer is capable of 0.1-nm resolution. However, for optimum signal-to-noise ratio it is generally operated at 0.4-nm resolution. Since the photon signal is low, photon-counting methods are employed. Electronic interfaces between the electron-impact collision chamber and uv spectrometer have been built. This interface synchron-

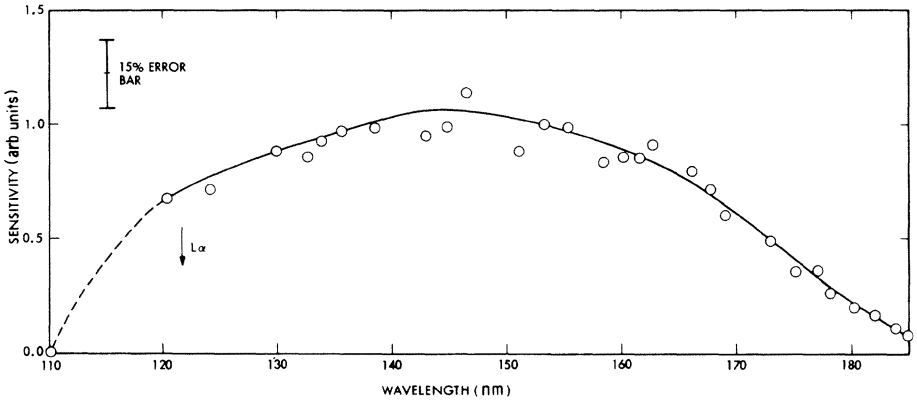

FIG. 1. Relative sensitivity of electron-impact emission spectrometer. The wavelength position of Lyman-α is indicated. The dashed line represents an estimated sensitivity.

izes the channel address in the multichannel analyzer with either the energy of the incident electron beam for the excitation function measurements or the wavelength for spectral scans. Thus, the apparatus can be operated either in "energy-scan" mode or in "wavelength-scan" mode, respectively.

Figure 2 shows a typical uv fluorescence spectrum obtained with the instrument in the wavelength-scan mode at 0.4-nm resolution taken at an electron-impact energy of 300 eV. The three important electronic transitions occurring in this region are indicated. They are the Werner-band system ($C\,^1\Pi_u \rightarrow X\,^1\Sigma_g^+$), the Lyman-band system ($B\,^1\Sigma_u^+ \rightarrow X\,^1\Sigma_g^+$) of H_2, and the Lyman-α transition ($2p \rightarrow 1s$). The $B \rightarrow X$ transition is complicated in that the transition is part continuum as described by Dalgarno *et al.*[24] and, additionally, is part cascade from the higher states.[4] The spectral region seriously affected by cascading is marked in Fig. 2. The primary cascade contribution involves the transition $E,F\,^1\Sigma_g^+ \rightarrow B\,^1\Sigma_u^+$. The Franck-Condon factors for cascading are quite different from those for direct excitation.[25,26] Thus the effects of cascading and direct excitation can be quantitatively separated since these processes preferentially populate different vibrational levels of the B state. On the other hand, for the $C\,^1\Pi_u$ state cascading does not appear to be important. Heaps *et al.*[19] have shown that cascading to the C state from the $G,P\,^1\Sigma_g^+$, $I,R\,^1\Pi_g$, and $J,S\,^1\Pi_g$ states has a less than 10% effect on the total cross section and that cascading does not, to first order, alter the population distribution among vibrational levels. Thus a measurement of a fraction of the band system will uniquely determine the extra emission in the extreme uv, which is not observed in this experiment.

The resolution of our optical system is 0.4 nm, a value sufficient to resolve vibrational but not rota-

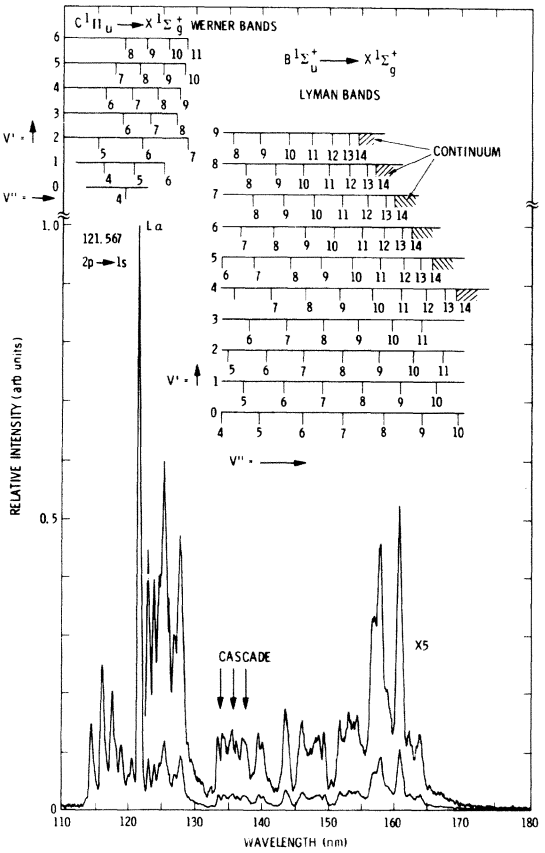

FIG. 2. Calibrated laboratory spectrum of H_2 at 300-eV electron-impact energy. The arrows indicate wavelength regions of strong cascading and continuum emission. The vibrational progressions of the Werner-band and Lyman-band systems are indicated. The spectral resolution is 0.4 nm.

tional structure. The vibrational bands are themselves quite wide due to the large rotational constant of H_2,[27] which causes band overlap with an approximate full width half maximum (FWHM) of about 0.5 nm. Thus it is necessary to include rotational structure in our synthetic spectrum model described in the Appendix. Stone and Zipf[6] have shown that the rotational structure can be resolved at 0.05-nm resolution.

No correction for polarization effects of the fluorescent radiation was made. The results presented here were measured at an angle of 90° between the electron-beam axis and the optic axis. Other excitation functions were measured at angles of 37° and 54.4°, the "magic" angle. These excitation functions were in agreement to within 10%, the experimental error. This result of the small variation of cross section with angle is to be expected, based on the polarization results of Malcolm *et al.*[13] These authors find that the effect of polarization on H_2 cross sections of Lyman- and Werner-band emissions at all impact energies is less than 25%.

III. EXPERIMENTAL RESULTS

We report in this section the results of emission cross-section measurements on the *B* and *C* states. These results are reported in the form of excitation functions measured from threshold to 400 eV, a table of absolute cross sections at 100 and 300 eV, and laboratory fluorescence spectra.

Figure 3 is a montage of electron-impact induced-fluorescence spectra between 110 and 170 nm at 0.4-nm resolution obtained at electron energies of 20, 100, and 300 eV. Each spectrum, consisting of 1024 data points on 0.1-nm centers, was best fitted in the least-squares sense with a model synthetic spectrum of the same resolution at 300-K rotational temperature, as described in the Appendix. By means of the synthetic spectrum the following three parameters were determined at each energy: (1) Q_A, the cascade cross section to the *B* state; (2) Q_B, the direct-excitation cross section of the *B* state; and (3) Q_C, the direct-excitation cross section of the *C* state.

The graphical comparison of the data and model for the 300-eV spectrum of Fig. 3 is shown in the lower half of Fig. 4. The resulting root-mean-square difference between data and model is 5%. The best-fit parameters Q_A, Q_B, Q_C are shown in Table I for 100 and 300 eV. For comparison we show in the upper part of Fig. 4 a two-parameter fit to the 300-eV spectrum for the case Q_A is set equal to zero. This synthetic spectrum clearly does not fit the laboratory spectrum as well as the synthetic spectrum in the lower half of Fig. 4, particu-

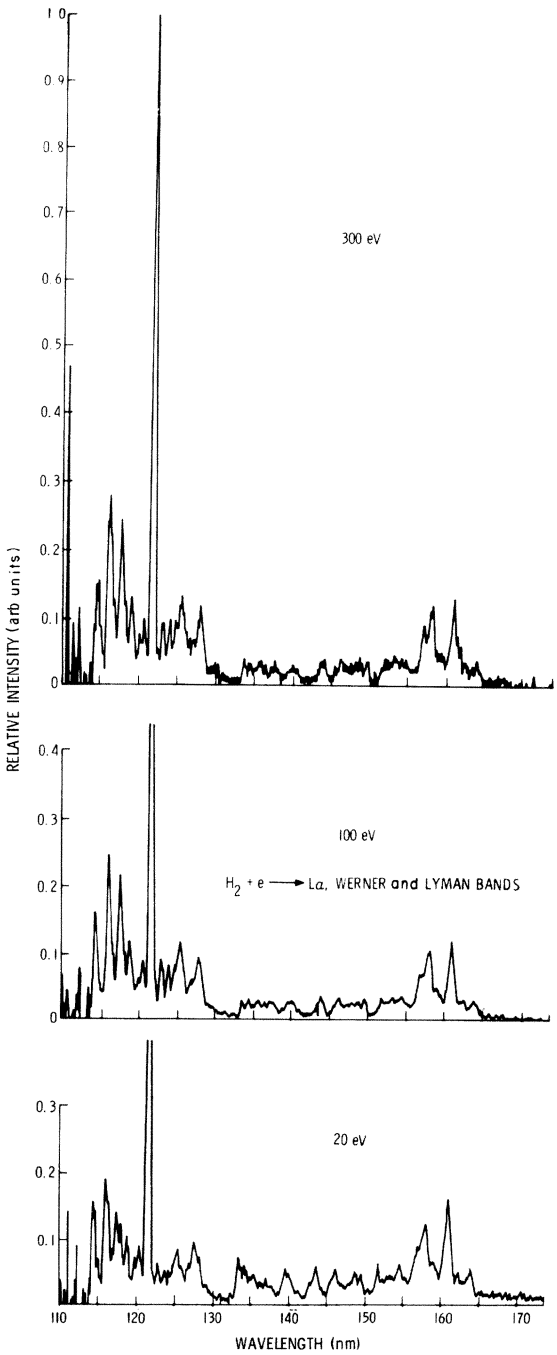

FIG. 3. Calibrated laboratory spectra of H_2 at 20, 100, and 300 eV at 0.4-nm resolution. The peak height of Lyman-α is normalized to unity at 121.57 nm.

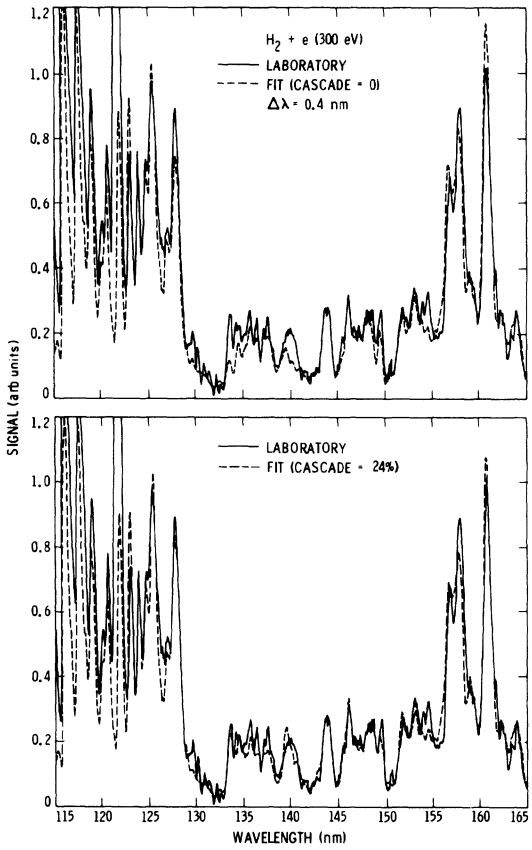

FIG. 4. Best fit to the laboratory data at 300 eV for the cases: (1) upper curve—cascade cross section is set equal to zero, (2) lower curve—cascade cross section is varied for best fit which in this case is found to be 24% of total emission cross section.

larly in the region of strong cascading from 130 to 145 nm. On the other hand, varying Q_A and Q_B to achieve the best fit does not effect the total emission cross section, $Q_A + Q_B$. In detail, the contribution from cascading comprises $24 \pm 10\%$ of the total emission cross section at both 100 and 300 eV. The uncertainty in the cascade contribution is indicative of the weak sensitivity of the models to cascading.

For comparison purposes, we show in Table I the values of recently measured and calculated cross-section values. We consider the *C/B* direct-excitation cross-section ratio one of the most important results of this study. For this reason we also show in Table I the *C/B* direct cross-section ratio as measured in this experiment and as determined from theory and other experiments. Our value of 1.21 ± 0.30 at 300 eV, which is the lower-energy edge of the Born-Bethe region,[1] agrees within 50% with theoretical and experimental *C/B* ratios deduced from generalized[28] and absorption[11] oscillator strengths.

A second important point to be considered in Table I is that we have the first simultaneous measurement of the *B*- and *C*-state cross sections including the *B*-state cascade contribution with the same optical system. A detailed comparison to the other determination of this ratio and to the cross sections in Table I will be made in Sec. IV. Suffice it to say, the agreement with theory is excellent for the *C* state (20% agreement), and fair for direct excitation of the *B* state (50% agreement).

We also measured certain vibrational bands of the *B* and *C* states as a function of electron energy. The results are displayed in Figs. 5 and 6 for the *B* and *C* states, respectively. The feature at 160.9 nm was chosen since it is the most intense *B-X* emission feature and because it has the smallest relative cascade contribution, e.g., 16% of measured signal at 100 eV based on our experimental values for cascading and direct excitation. We show in Sec. IV that, for energies below 30 eV, the importance of the cascading process increases rapidly with decreasing energy and that the measured 160.9-nm excitation function in Fig. 5 includes a 34% contribution from cascading at 20 eV. In the case of the *C* state, the (5,12) band at 124.9 nm was studied since this feature contains a very small contribution from the Lyman-band system. In Table II we summarize the relative energy dependences of the cross sections for the *B* and *C* states based on the results of the excitation function measurements for the two vibrational bands. As mentioned, the *B*-state energy dependence includes the effects of cascading. However, the effect of cascading on the energy dependence (relative shape of curve) is shown to be less than 10% for impact energies greater than 30 eV. On the other hand, the *C*-state values are expected to be free of cascading and to represent without correction the direct-excitation cross-section energy dependence.

We find a peak *B*-state cross section at $35-40$ eV. The measured relative cross-section shape (including cascade) agrees closely with the semiempirical calculations of Gerhardt[14] (cascade free) and the excitation function measurements of Malcolm *et al.*[13] (with cascade). A couple of theoretical direct-excitation cross-section calculations, for example, those by Fliflet and McCoy[5] also shown in Fig. 5, have found a *B*-state cross-sectional energy dependence that correctly predicts the shape. The good agreement between present results and experimental values of Malcolm *et al.*[13] and cascade-free

TABLE I. (a) Absolute emission cross sections and the C/B cross-section ratio of H_2. (b) The ratio C/B cross section for direct excitation.[a]

	Transition	Cross section (10^{-17} cm^2)									
		(a)									
		100 eV									
		b	c	d	e	f	g	h	i	j	k
Q_A	$B\,^1\Sigma_u^+ \rightarrow X\,^1\Sigma_g^+$ (cascade)							0.85	0.43	0.38	
Q_B	$B\,^1\Sigma_u^+ \rightarrow X\,^1\Sigma_g^+$ (direct)	4.3			3.6		3.9	2.7	3.3		2.6
Q_C	$C\,^1\Pi_u \rightarrow X\,^1\Sigma_g^+$ (total=direct)	4.8	3.2	2.7		5.3	3.0	3.1	3.5		
		300 eV									
		b	c	d	e	f	g	h	i	j	k
Q_A								0.45	0.15	0.12	
Q_B		2.2						1.4	1.6		2.2
Q_C		2.7	1.9	1.6		2.9		1.7	1.8		

(b)

	l	m	n	o	p	q	r
From Theor. f values				1.02			
From Expt. f values		0.86					
Theor. cross section	1.23				0.85		1.08
Expt. cross section			0.82			1.21	

[a]The cross-section ratio, C/B, from oscillator strength measurements (l,m,n) uses the Born-Bethe approximation and constants given in Ref. 14.
[b]Gerhardt (Ref. 14) (Theor. + Expt.).
[c]DeHeer and Carriere (Ref. 1) (Expt.), Allison and Dalgarno (Ref. 12) (Theor.).
[d]DeHeer and Carriere (Ref. 1) (Expt.), Fabian and Lewis (Ref. 11) (Expt.).
[e]Chung and Lin (Ref. 2) (Theor.).
[f]Stone and Zipf (Ref. 6) (Expt.).
[g]Fliflet and McCoy (Ref. 5) (Theor.); Lee and McCoy (Ref. 3).
[h]This work (Expt.).
[i]Arrighini *et al.* (Ref. 4) (Theor.).
[j]Fajen (Ref. 16) (Theor.).
[k]McConkey (Ref. 18) (Expt.).
[l]Gerhardt (Ref. 14) (300 eV).
[m]Fabian and Lewis (Ref. 11).
[n]Geiger and Schmoranzer (Ref. 28) (34 keV).
[o]Allison and Dalgarno (Ref. 12).
[p]Lee and McCoy (Ref. 3), Fliflet and McCoy (Ref. 5) (100 eV).
[q]This work (300 eV).
[r]Arrighini *et al.* (Ref. 4) (300 eV).

theoretical calculations shown in Fig. 5 indicate that at electron-impact energies above 30-eV cascading does not affect the energy dependence. The absolute values for the cross section of the B state are compared in Sec. IV.

Although absolute cross-section values for C state do not agree with Stone and Zipf,[6] we find that the relative shapes (Fig. 6) of the excitation function curves agree well. The relative energy dependence agrees within the 10% error bars of each experiment. The results of Stone and Zipf are important in that they represent the only previous experimental emission cross-section work including the threshold region. The theoretical results of Arrighini *et al.*[4] using the first-Born approximation are also shown. These authors have also calculated direct-excitation cross sections to several other electronic states including the B state.

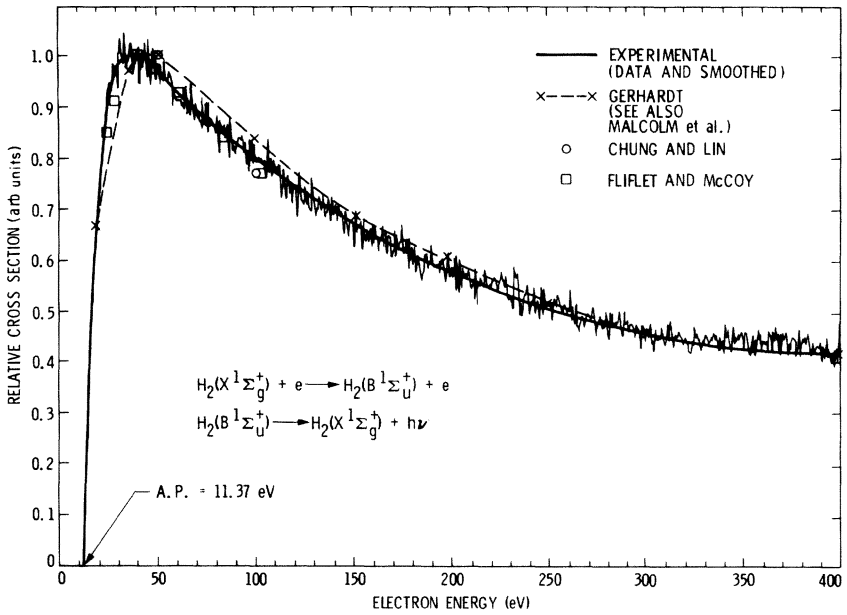

FIG. 5. Relative-emission cross section of 160.9-nm Lyman-band feature obtained with instrument in energy-scan mode. The instrument band pass of 0.6 nm was centered on the (5,12) vibrational band at 160.9 nm and includes contributions from other transitions. The literature values are normalized to unity at the energy corresponding to their peak cross section.

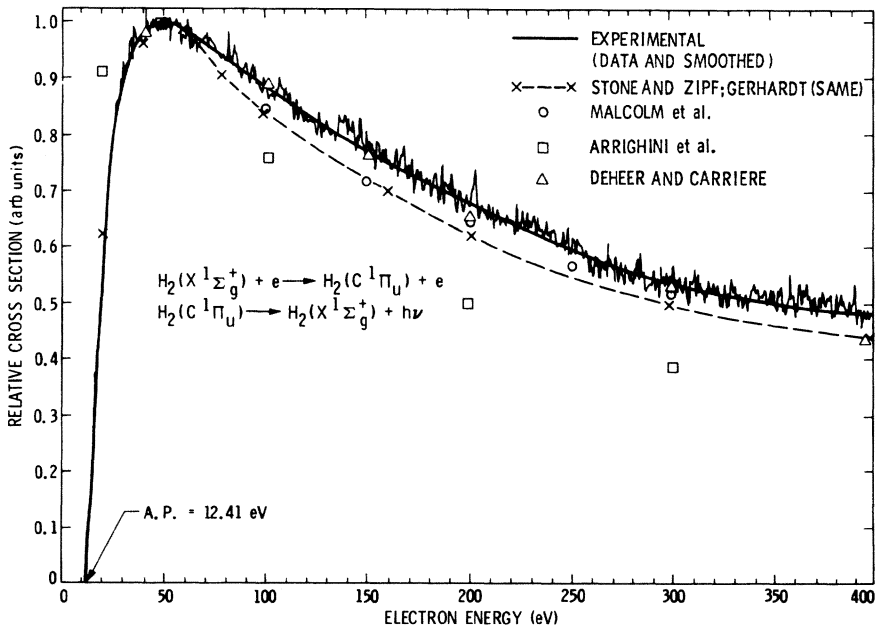

FIG. 6. Relative-emission cross section of Werner bands. The instrument band pass of 0.6 nm was centered on the (5,9) band at 124.9 nm. The literature values are normalized to unity at the energy corresponding to their peak cross section.

TABLE II. Measured relative-emission cross sections of H_2 for excitation of the $B\ ^1\Sigma_u^+$ and $C\ ^1\Pi_u$ states based on the energy dependence of the 160.9 and 124.9 nm vibrational features, respectively.

Energy (eV)	Relative-emission cross section[a] $B\ ^1\Sigma_u^+$ (arb. units)	Relative-emission cross section $C\ ^1\Pi_u$ (arb. units)
15	0.30	0.30
20	0.69	0.60
25	0.90	0.87
30	0.97	0.92
40	1.0	0.98
50	0.98	1.0
60	0.93	0.99
70	0.90	0.97
80	0.86	0.94
90	0.83	0.91
100	0.80	0.88
120	0.74	0.83
150	0.67	0.76
200	0.58	0.67
250	0.50	0.59
300	0.45	0.53
400	0.41	0.48

[a]This column lists the excitation function of the 160.9-nm feature which includes a small amount of cascading. The contribution from cascading is calculated and the direct-excitation relative-emission cross section is presented in Table III.

IV. DISCUSSION

From a fundamental point of view an important result of this study is the comparison in Table I between the laboratory measured *C/B* direct-excitation cross-section ratio at 300 eV and the calculated *C/B* direct-excitation cross-section ratio from *C/B* oscillator strength determinations, using the Born-Bethe approximation.[1,14] We are finding good agreement between our experimental ratio at 300 eV when compared to theoretical and experimental values for the ratio based on oscillator strengths. This 50% agreement is shown in Table I. In particular, we are finding good agreement between our results and the theoretical calculations of Allison and Dalgarno.[11] These authors calculated individual band oscillator strengths of the *B* and *C* states based on electronic transition moment functions and vibrational wave functions.

The experimental data by Fabian and Lewis[11] indicate the $(v',0)$ band oscillator strengths of Allison and Dalgarno[12] may be too high by as much as 20% at small v'. Our cross-section value for the *C* state was derived by estimating the short-wavelength emission for the Werner bands, part of which comes from small v', from the Allison and Dalgarno band oscillator strengths. Thus the experimental value of 1.21 for the *C/B* ratio and the *C*-state cross-section values in Table I may be biased high by about 10%. A 10% reduction in the *C/B* ratio, for example, clearly makes better agreement with the other theoretical and experimental values listed in Table I. A more exact treatment would require a recalculation of transition probabilities of the Werner-band system based on the Fabian and Lewis experimental results for use in our synthetic modeling code.

From another point of view, there appears to be a strong evidence that the experimental results of Stone and Zipf[6] are too high by 70% for the *C* state even including corrected modeling of their rotational bands (see Appendix). On the other hand, it is difficult to assign an accurate total electronic cross-section value to the Stone and Zipf's work, which only measured a few individual rotational cross sections and emphasizes the importance of summing individual rotational cross sections over all rotational lines of many vibrational bands, as was done here. The next step, of course, is to actually measure the total emission "count all the photons" from the Werner-band system, taking into proper account of the other uv band systems that have recently been found to exist in emission in the short-wavelength spectral region,[29] e.g., *B'*, *B''*, *D*, and *D'*. In detail, these bands span the wavelength range 80—110 nm and overlap with the Werner system. These bands, however, do not affect our analysis presented here.

Furthermore, the experimental results of deHeer and Carriere[1] for the *C* state based on the Born-Bethe approximation and available oscillator strengths and the theoretical results of Arrighini *et al.*[4] for the *C* state agree to within 20% to our absolute values at 100 and 300 eV. This agreement is shown in Table I. Accordingly, our experimental results for the *C*-state cross section and the *C/B* ratio points out that theoretical cross-section calculations for the *B* state at 100 and 300 eV appear in general too large by about 50%. The theoretical estimates for the *B* state are shown in Table I. Many different *ab initio* approximations (distorted-wave, close-coupling and Born approximation) are attempted with good internal agreement among the various theoretical approaches.

Our results at high energy for cascading to the *B*

state are higher than previous theoretical predictions but the uncertainty in the cross section for cascading in Table I is large by about 40%. Thus our results do not preclude the theoretical results as a lower limit. These theoretical cross sections at 100 and 300 eV for cascading[4,16] are about a factor of 2 smaller than our best-fit value and indicate a 10—15% contribution to the total emission cross section from cascading.

A fundamental point in the consideration of H_2 excitation by electrons deals with the effects of cascading, particularly at low energies. We have shown that cascading is an important effect at 100 and 300 eV for the B state, contributing $24\pm10\%$ of the total emission cross section at these energies. The important cascade contributing states arise from the degenerate E and F states of configurations $[1s\sigma,\ 2s\sigma+(2p\sigma)^2]$. The two-step cascade transition to the B state follows the scheme:

$$H_2(X\,^1\Sigma_g^+)+e\rightarrow H_2(E,F\,^1\Sigma_g^+)\ , \tag{1}$$

$$H_2(E,F\,^1\Sigma_g^+)\rightarrow H_2(B\,^1\Sigma_u^+)+h\nu\ . \tag{2}$$

Other contributing states including the $H\,^1\Sigma_g^+(1s\sigma)(3s\sigma)$ state have been shown to yield an exceedingly small[4] cascade contribution relative to the E,F states contribution at all impact energies. For example, Arrighini *et al.*[4] calculate the H-state cross section to be about 0.5% of the E,F states at 300 eV. Also, the results of Day *et al.*[30] indicate the cross section of the $G\,^1\Sigma_g^+(1s\sigma)(3d\sigma)$ state is small compared to the E,F states. This rapid fall-off in cross section with principal quantum number is expected since the oscillator strength varies as the inverse cube of the principal quantum number.[31]

The optical excitation function for the E,F states has been measured by Watson and Anderson[17] and calculated theoretically by Fajen[16] and Arrighini *et al.*[4] Equation (1) shows a magnetically allowed dipole transition. The E,F cross section[4,16,17] is sharply peaked in the threshold region, 20—25 eV, falling to $\frac{1}{3}$ to $\frac{1}{6}$ the peak value at 100 eV. This shape arises because of the nature of the $g\rightarrow g$ transition which is an electrical-dipole forbidden transition. Consequently we expect cascading to be more important at low energies. We have measured the H_2 fluorescent spectrum at 20 eV as shown in bottom panel of Fig. 3. The difference in relative-band intensities between the 20-eV spectrum, on one hand, and the 100- and 300-eV spectra, on the other, is quite dramatic for the $B\rightarrow X$ transition. For that reason we have magnified the 20- and 100-eV spectra of Fig. 3 and show them again in Fig. 7. The important cascading transitions, namely, the members of the $v'=0$ progression, are clearly enhanced in the 20-eV spectrum over those of the higher-energy spectrum.

The least-squares fit to the 20-eV spectrum indicates that the cross sections are $Q_A=1.75\times10^{-17}$ cm^2 (cascade), $Q_B=1.68\times10^{-17}$ cm^2 (direct), and $Q_C=1.56\times10^{-17}$ cm^2 (direct). Thus, at 20 eV there is almost equal contribution to the Lyman-band total emission from cascading and direct excitation. The value for Q_B compares very favorably to the electron scattering value of $(1.9\pm0.6)\times10^{-17}$ cm^2 at 20 eV measured by Srivastava and Jensen.[15] At the same time our value for Q_A is close to the theoretical value of 1.3×10^{-17} cm^2 predicted by Fajen and consistent with the lower-limit value of 1.2×10^{-17} cm^2 measured by Watson and Anderson.[17] Our result, however, is significantly larger than the result of 5×10^{-18} cm^2 predicted by Arrighini *et al.*[4]

Heaps *et al.*[19] have shown that cascading will most strongly populate the $v'=0$ level, which compares with the $v'=6,7$ levels for the case of direct excitation. The most intense cascade band on the basis of calculation is expected to be the (0,4) band at 133.4 nm, which is clearly the case in the laboratory spectrum at 20 eV. Other enhanced features occur at 127.5 nm (0,3), 139.4 nm (0,5), 145.6 nm (0,6), and 151.7 nm (0,7).

The preceding discussion shows that the vibrational population distribution of the B state will vary with energy. In Fig. 8 we plot the relative vibrational population of the $B\,^1\Sigma_u^+$ state at 20 and 100 eV. Electrons of low-impact energies ($\epsilon<30$ eV) will excite the B state in a manner to populate the low-vibrational levels the most, beginning at $v'=0$, while electrons of high-impact energies ($\epsilon>30$ eV) will favor direct excitation and will shift the peak population distribution to $v'=6$.

The experimental results of Watson and Anderson[17] show that the cascade cross section falls by a factor of 6 and the theoretical results of Fajen[16] indicate that the cascade cross section falls by a factor of 3.5 between the peak value near 20 and 100 eV. Our results indicate that the E,F state cross section decreases by a factor of 2.1 between 20 and 100 eV. We have used our experimental results already discussed at 20, 100, and 300 eV, together with a result obtained at 50 eV

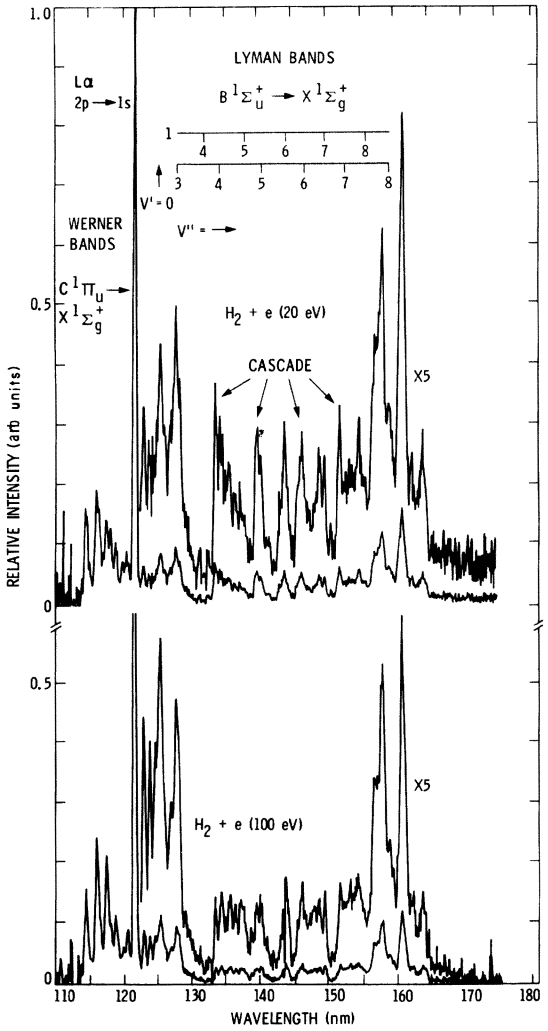

FIG. 7. Calibrated electron-impact fluorescent spectra of H_2 at 20 and 100 eV. A 5× magnification inset is also shown. These are the same spectra as shown in Fig. 3.

($Q_A = 0.93\times10^{-17}$ cm^2, $Q_B = 3.11\times10^{-17}$ cm^2, $Q_C = 3.09\times10^{-17}$ cm^2) and, for interpolation between energies, the excitation function measurement of the E state by Watson and Anderson.[17] This procedure enabled us to determine the effects of cascading on the B-state excitation function results of Table II. For example, the cascade contribution at 160.9 nm according to our synthetic spectrum model and experimental cross-section results is the following: (1) 20 eV, cascading is 34%, (2) 100 and 300 eV, cascading is 16%. The relative numerical values for direct excitation from 20 to 300 eV for the $B\,^1\Sigma_u^+$ state are given in Table III to 20% accuracy.

We see the difference in the cross-section values

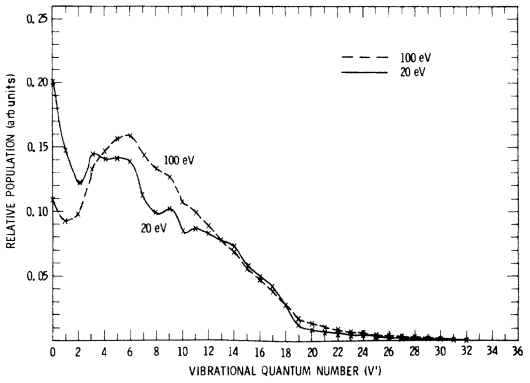

FIG. 8. Vibrational population of the $B\,^1\Sigma_u^+$ state of H_2 at electron-impact energies of 20 and 100 eV based on our experimental cross sections for direct excitation and cascading.

given in Tables II and Table III for the energy dependence of the B-state cross section is small (10% or less) for $\epsilon > 30$ eV. It is not fruitful to extrapolate below 20 eV since the change in cross section[17] for the E state is quite rapid with energy. The 2-eV uncertainty between the results of Watson and Anderson and the results presented here would lead to extremely large uncertainties in cross-section values below 20 eV. For comparison, we show in Fig. 9, some of the recent relevant experimental and theoretical cross-section results for direct excitation of the B state. Note the magnitude of the three experimental values tend to be about 50% lower than the theoretical values. The energy dependence recently measured by McCon-

TABLE III. Relative-emission cross section of H_2 for direct excitation of the $B\,^1\Sigma_u^+$ state.

Energy (eV)	Relative-emission cross section $B\,^1\Sigma_u^+$ (arb. units)
20	0.51
25	0.79
30	0.94
40	1.0
50	0.99
60	0.94
70	0.91
80	0.88
90	0.85
100	0.82
150	0.71
200	0.61
250	0.52
300	0.47

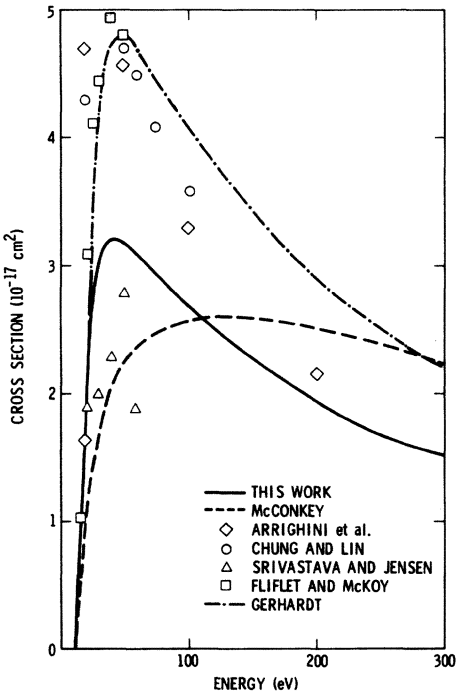

FIG. 9. Direct-excitation cross section of the B state of H_2 from the literature and from this work.

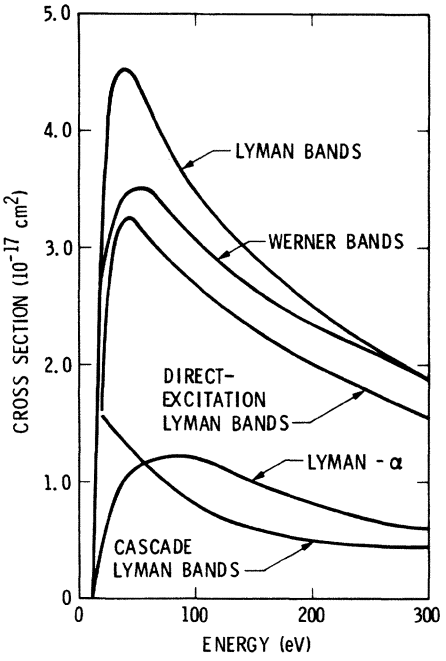

FIG. 10. Important cross sections for electron-impact excitation of H_2 based on this work for the B and C states and on the work of Mumma and Zipf (Ref. 20) for Lyman-α.

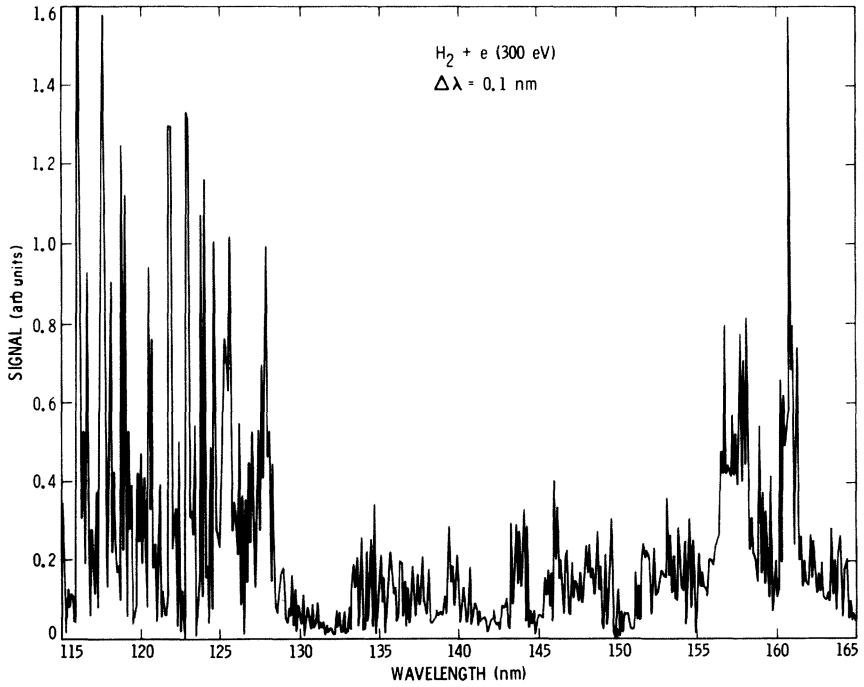

FIG. 11. Synthetic spectrum of H_2 at 0.1-nm resolution and 300-eV impact energy. The relative intensities of each band system including the cascade contribution to the B state are based on our results for Q_A, Q_B, and Q_C.

key[18] is quite different than that measured here though the absolute values agree to 30%. The difference may arise from the fact McConkey assumed the cascade contribution goes to zero at 300 eV.

Finally, we have summarized on an absolute scale all our results (except for Lyman-α) for H_2 in Fig. 10. For the sake of completeness we have added the Lyman-α result of Mumma and Zipf.[20] The cross section with the largest uncertainty (50%) is the cascade contribution to the B state. On the other hand, the emission cross-section values of the Lyman- and Werner-band systems are accurate to 20%. Note the approximate 5-eV difference in peak cross section between the direct-excitation cross section of the B state and the emission cross section of the B state. This shift does not appear in the 10-eV intervals of Tables II and III. Additionally it should be noted that the relative values for the direct-excitation cross sections at 20, 50, 100, and 300 eV obtained by the least-squares technique evaluation of the total emission intensity (Table I and Sec. IV) agree to within 10% to those obtained from the excitation function measurements of individual vibrational bands (Tables II and III).

ACKNOWLEDGMENT

This work was supported by the Planetary Atmospheres, Astronomy/Relativity and Laser Kinetics Programs of NASA. It represents one phase of work sponsored by NASA under Contract No. NAS7-100 to the Jet Propulsion Laboratory, California Institute of Technology, Pasadena, California 91109.

APPENDIX

Synthetic spectra

First we generate individual synthetic H_2 emission spectra due to the Lyman system, the Werner system, and the cascade populated Lyman system. In these calculations, we assume that the vibrational levels of the upper states are populated in steady state according to the weighting function

$$\omega(v') = C\lambda_{v',0}^{3} A_{v',0} ,$$

where C is a normalization constant, $\lambda_{v',0}$ and $A_{v',0}$ are, respectively, the appropriate wavelength and the transition probability between the v'th vibrational level of the upper state and the ground state $X\,^1\Sigma_g^+$, $v''=0$. The distribution of intensity in the rotational structure of each band is calculated with the Honl-London factors, assuming that the ground-state rotational levels are populated by a Boltzmann distribution at room temperature (see, for example, Herzberg,[27] Stone and Zipf[6]). There is a minor error in Stone and Zipf[6] in calculating the rotational population. In exciting the Werner bands, the transitions are $X\,^1\Sigma_g^+$, $v''=0 \rightarrow C\,^1\Pi_u$, $v' \rightarrow X\,^1\Sigma_g^+$, v''. The rotational population refers to the initial state $X\,^1\Sigma_g^+$, $v''=0$, but Stone and Zipf inadvertently used the population of the final state $X\,^1\Sigma_g^+$, v''. This introduces about 20% error in their analysis. The relevant molecular physics data for $X\,^1\Sigma_g^+$, $B\,^1\Sigma_u^+$, and $C\,^1\Pi_u$ states are taken from Herzberg and Howe,[32] Allison and Dalgarno,[12] Mofils,[33] and Huber and Herzberg.[34] In synthesizing the spectrum of Lyman continuum emission,[24]

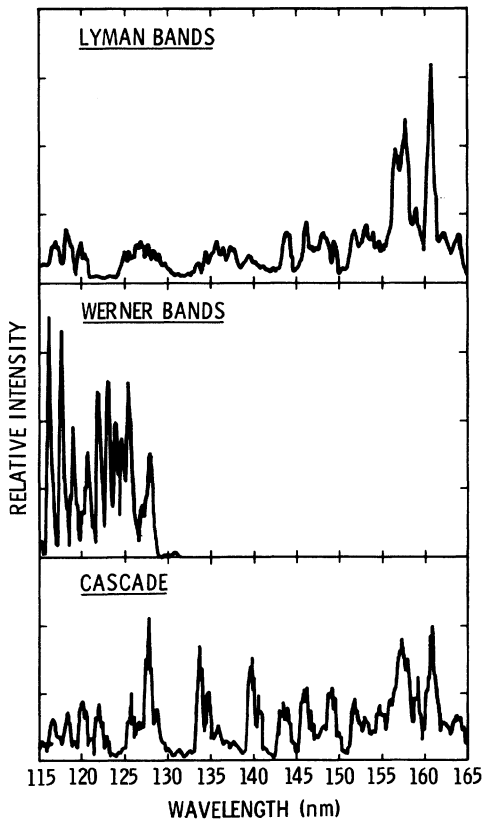

FIG. 12. Synthetic spectra of H_2 showing: (1) upper curve, direct-excitation spectrum of Lyman-bands continuum + discrete transitions, (2) middle curve, Werner bands, (3) lower curve, cascading of the B state.

we use the matrix elements tabulated by Stephens.[35] For computing cascading from $E,F\,^1\Sigma_g^+$ states we take the Franck-Condon factors from Lin.[26] The raw synthetic spectra are then degraded to the experimental resolution using 0.4-nm running averages. To obtain a parametrized fit to the laboratory spectrum, we assume that the cross section for Lyman-$\alpha = 1.2\times10^{-17}$ cm^2 and that the cross sections for direct excitation $B\,^1\Sigma_u^+$, $C\,^1\Pi_u$, and $B\,^1\Sigma_u^+$ via cascade are unknown parameters, to be determined by a nonlinear least-squares fitting program. The procedure is straightforward, and yields high-quality fits to the data with root-mean-square error in the range of 5% or less. We show in Fig. 11 a synthetic spectrum at high resolution of 0.1 nm and the complexity of the rotational structure is clearly indicated. Subsequently in Fig. 12 we show the individual Lyman-band system, the Werner-band system, and the cascading contribution to the Lyman-band system at our experimental resolution of 0.4 nm. The relative intensities within any one band system are independent of the results presented here. The figure shows that the measured signal intensity at low resolution in the vuv contains contributions from both cascade and direct excitation at virtually every wavelength.

An important question we have to consider is, how unique are the least-squares fits? We make a number of sensitivity tests such as varying averaging of the raw synthetic spectra from 0.3 to 0.5 nm, and fixing the ratio of the cascade to direct excitation of the Lyman system. The results of such tests indicate that our cross sections Q_B and Q_C have been fairly uniquely determined. The error in Q_A as already discussed, is, however, large and is about 40%. The physical reason for the success of such a simple analysis is that, to first order, the Lyman emissions dominate the spectral region longward of 140.0 nm, the Werner emissions dominate the short wavelength emissions between Lyman-α and 130 nm, and the cascade contributions to Lyman emissions are most prominent between 130 and 150 nm.

[1]F. J. deHeer and J. D. Carriere, J. Chem. Phys. 55, 3829 (1971).

[2]S. Chung and C. Lin, Phys. Rev. A 17, 1874 (1978).

[3]M. T. Lee and V. McKoy (unpublished).

[4]G. P. Arrighini, F. Biondi, C. Guidotti, A. Biagi, and F. Marinelli, Chem. Phys. 52, 133 (1980).

[5]A. W. Fliflet and V. McKoy, Phys. Rev. A 21, 1863 (1980); A. Hazi, Phys. Rev. A 23, 2232 (1981).

[6]E. J. Stone and E. C. Zipf, J. Chem. Phys. 56, 4646 (1972).

[7]A. L. Broadfoot, M. J. S. Belton, P. Z. Takacs, B. R. Sandel, D. E. Shemansky, J. B. Holberg, J. M. Ajello, S. K. Atreya, T. M. Donahue, H. W. Moos, J. L. Berteaux, J. E. Blamont, D. F. Strobel, J. C. McConnell, A. Dalgarno, R. Goody, and M. B. McElroy, Science 204, 979 (1979).

[8]B. R. Sandel, D. E. Shemansky, A. L. Broadfoot, J. L. Berteaux, J. E. Blamont, M. J. S. Belton, J. M. Ajello, J. B. Holberg, S. K. Atreya, T. M. Donahue, W. H. Moos, D. F. Strobel, J. C. McConnell, A. Dalgarno, R. Goody, M. B. McElroy, and P. Z. Takacs, Science 206, 962 (1979).

[9]J. T. Clarke, H. W. Moos, S. K. Atreya, and A. L. Lane, Astrophys. J. Lett. 241, L179 (1980).

[10]Y. L. Yung, G. R. Gladstone, K. M. Chang, J. M. Ajello, and S. K. Srivastava, Appl. J. Lett. (in press).

[11]W. Fabian and B. W. Lewis, J. Quant. Spectrosc. Radiat. Transfer 14, 523 (1974).

[12]A. C. Allison and A. Dalgarno, At. Data 1, 289 (1970).

[13]I. C. Malcolm, H. W. Dassen, and J. W. McConkey, J. Phys. B 12, 1003 (1979).

[14]D. E. Gerhardt, J. Chem. Phys. 62, 82 (1975).

[15]S. K. Srivastava and S. Jensen, J. Phys. B 10, 3341 (1977).

[16]F. E. Fajen, Ph.D. dissertation, University of Oklahoma, Norman, Okla., 1968 (unpublished).

[17]J. Watson and R. J. Anderson, J. Chem. Phys. 66, 4025 (1977).

[18]J. W. McConkey, J. Chem. Phys. 74, 6224 (1981).

[19]M. G. Heaps, J. N. Bass, and A. E. S. Green, Icarus 24, 78 (1975).

[20]M. J. Mumma and E. C. Zipf, J. Chem. Phys. 55, 1661 (1971).

[21]J. M. Ajello and S. K. Srivastava, J. Chem. Phys. 75, 4454 (1981).

[22]M. J. Mumma, J. Opt. Soc. Am. 62, 1459 (1972).

[23]M. J. Mumma and E. C. Zipf, J. Opt. Soc. Am. 61, 83 (1971).

[24]A. Dalgarno, G. Herzberg, and T. L. Stephens, Astrophys. J. Lett. 162, L49 (1975).

[25]R. J. Spindler, J. Quant. Spectrosc. Radiat. Transfer 9, 627 (1969).

[26]C. S. Lin, J. Chem. Phys. 60, 4660 (1974).

[27]G. Herzberg, *Molecular Spectra and Molecular Structure I, Spectra of Diatomic Molecules* (Van Nostrand Reinhold, New York, 1950), pp. 658.

[28]J. Geiger and H. Schmoranzer, J. Mol. Spectrosc. 32,

39 (1969).
[29]J. M. Ajello, S. K. Srivastava, and Y. Yung, EOS, 62, 940 (1981); J. M. Ajello, S. K. Srivastava, Y. L. Yung, and D. Kwok (unpublished).
[30]R. L. Day, R. J. Anderson, and F. A. Sharpton, J. Chem. Phys. 71, 3683 (1979).
[31]W. T. Miles, R. Thompson, and A. E. S. Green, J. Appl. Phys. 43, 678 (1972).
[32]G. Herzberg and L. L. Howe, Can. J. Phys. 37, 636 (1959).
[33]A. Monfils, J. Mol. Spectrosc. 25, 513 (1908).
[34]K. P. Huber and G. Herzberg, *Molecular Spectra and Molecular Structure IV, Constants of Diatomic Molecules* (Van Nostrand Reinhold, New York, 1979), pp. 716.
[35]T. L. Stephens, Ph.D. thesis, Harvard University, 1970 (unpublished).